Vibrational Analysis And Molecular Docking Studies Of (S) 5-Methoxy-2-[(4-Methoxy-3, 5-Dimethylpyridin-2-Yl)Methylsulfinyl]-3H-Benzoimidazole

K.Shobana, E.Sailatha, S. Gunasekaran, P.Rajesh, S. Srinivasan, M.Raja, P.P.Moorthi

Abstract: The solid phase FTIR and FT-Raman spectra of (S) 5-Methoxy-2-[(4-methoxy-3, 5-dimethylpyridin-2-yl)methylsulfinyl]-3H-benzoimidazole (abbreviated as S5M4M35DM3B) have been recorded in the regions 4000-450 and 4000-50cm^{-1} respectively. The assignments of the vibrational spectra have been carried out with the aid of potential energy distribution (PED). The charge delocalization and Stability of the molecule arising from hyperconjugative interactions have been calculated using natural bond orbital (NBO) analysis. UV-visible spectrum was recorded using DMSO as solvent and its electronic properties HOMO and LOMO energies were calculated. ^{1}H and ^{13}C NMR chemical shift of the molecule were calculated. The Fukui function was calculated to explain the chemical reactivity site in S5M4M35DM3B. The molecular electrostatic potential (MEP) and other molecular properties were calculated and discussed. The Molecular docking studies were made to determine target protein.

Keywords: DFT, UV, FTIR, FT Raman spectra, NPA, NBO, Fukui function

1. INTRODUCTION

The Nonsteroidal anti-inflammatory drugs (NSAIDs), which are most commonly used drugs worldwide. However, they are associated with a substantial risk of upper gastrointestinal adverse events, ranging from ulcers to serious ulcer complications such as perforation, obstruction and bleeding[1]. Proton pump inhibitors have well-documented efficacy for reducing the incidence of NSAID-associated endoscopic ulcers and upper gastrointestinal symptoms[2], and are recognized as an effective gastroprotective strategy for at-risk patients[3]. (S)5-Methoxy-2-[(4-methoxy-3,5-dimethylpyridin-2-yl)methylsulfinyl]-3H-benzoimidazole(S5M4M35DM3B) is a proton pump inhibitor with effective gastric acid suppression.S5M4M35DM3B is the S-isomer of omeprazole, which is a mixture of the S- and R-isomers.The molecular formula is $C_{17}H_{19}N_3O_3S$. S5M4M35DM3B is used to treatcertain stomach and esophagus problems (such as acid reflux, ulcers). It works by decreasing the amount of acid your stomach produces. It is also used in the treatment of diseases like dyspepsia, peptic ulcer disease, gastroesophageal reflux disease and Zollinger-Ellison syndrome.

The literature survey shows that there were quantum studies done for this molecule so far. The complete experimental spectroscopic investigation on the molecule like FT-Raman, FT-IR and UV–vis methods has done. The density functional theory (DFT) calculations by the B3LYP method using 6-31G(d,p) basis set by Gaussian 03 Program, the quantum characters were studied. The intermolecular interactions and stability of can be determined by natural bond orbital analysis (NBO). The UV–vis spectrum gives with maximum absorption of the molecule and we can find HOMO and lowest unoccupied molecular orbital energy LUMO and finally, the band gap energy can be used to determined. By using the band gap value, the electronic properties like electron affinity, chemical hardness and chemical softness of the molecule has been obtained. The charge transfer and the molecular structure of the title molecule is obtained by molecular electrostatic potential (MEP) and Fukui function analysis. Finally, the molecular docking studies provide the interaction of the titled compound with different proteins explains the good antiulcer properties.

2. Experimental Details

The Pharmaceutical drug compound S5M4M35DM3B in the powder form was procured from the reputed chemical company in Pondicherry, India and used as such without further purification. The FT-IR spectrum of the sample is recorded in the region 4000-450cm^{-1} using KBr pellet technique with 4cm^{-1} resolution on a PERKIN ELMER FT-IR Spectrometer at SAIF, St.Peter's University, Chennai, India. The FT-Raman spectrum was recorded with 1064nm line of Nd:YAG laser as excitation wavelength in the region 4000-50cm^{-1} using Bruker RFS 27 Spectrometer with at a resolution of 2cm^{-1} at SAIF, IIT, Chennai, India. The Ultra Violet-Visible absorption spectrum was examined in the range 200-400nm using Varian Cary 5E-UV-NIR Spectrometer at IIT, Chennai, India. All the measurements were recorded in room temperature.

- *Department of Physics, Pachaiyappa's college, Tamilnadu, India.*
- *Department of Physics,School of Basic Sciences, Vels Institute of Science Technology & Advanced Studies (VISTAS), Pallavaram, Chennai, 600 117, Tamilnadu, India.*
- *Research & Development,St.Peter'sUniverisity, Avadi, Chennai, Tamilnadu, India.*
- *Department of Physics, PresidencyCollege, Chennai, Tamilnadu, India.*
- *Department of Physics, Jamal Mohamed College,*

3. COMPUTATIONAL DETAILS

The geometry of S5M4M35DM3B was fully optimized using density functional theory (DFT), B3LYP exchange correlation functional and 6-31/G (d,p) [4,5] with Gaussian 03 program package[6]. The UV-Visible spectra, electronic transitions and other electronic properties such as HOMO, LUMO and Energy gap were computed with the help of time-dependent DFT (TD-DFT) method. The HOMO and LUMO analysis have been used to elucidate the information regarding the charge transfer within the molecule. To confirm the vibrational band assignments potential energy distribution (PED) calculation was carried out by the VEDA (Vibrational Energy Distribution Analysis) program [7].

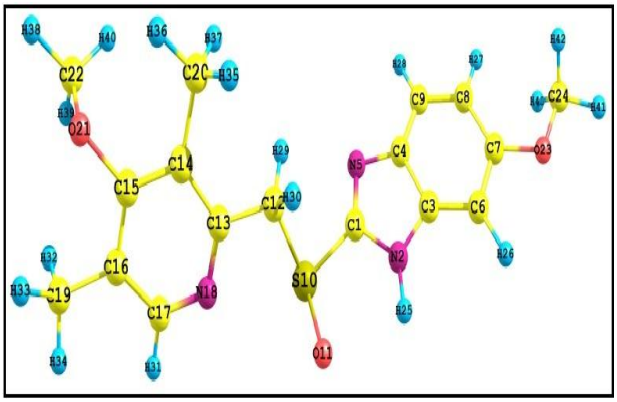

Fig.1 *Optimized structure of S5M4M35DM3B*

4. RESULTS AND DISCUSSION

4.1 Molecular geometry

The molecular structure of S5M4M35DM3Balong with numbering of atoms is shown in Fig 1.From the structural point of view, the title molecule consists of 43 atoms, hence undergoes 123 normal modes of vibrations and hence, belongs to C1 point group symmetry. All the calculated frequency contained to the same symmetry species. The optimized geometrical parameters (bond lengths and bond angles)obtained by the DFT calculations are presented in Table 1.The DFT calculation gives shortening of angles like (C1-S10-C12)93.598, (C1-N5-C4)103.80, (N2-C3-C4)104.54 and increase of angles like (C16-C17-N18)124.16, (N5-C4-C9)130.32, (N2-C3-C6)132.59. The bond lengths such as S10-C12 1.8552, (C12-C13)1.5108, (C16-C19)1.5061

Table 1. Geometrical parameters ofS5M4M35DM3B

Bond length(Å)	B3LYP/6-31G(d,p)	Bond angle (^{0})	B3LYP/6-31G(d,p)
C_1-N_2	1.3699	O_2-C_1-N_5	114.87
C_1-N_5	1.3054	N_2-C_1-S_{10}	116.62
C_1-S_{10}	1.8159	N_5-C_1-S_{10}	128.32
N_2-C_3	1.3824	C_1-N_2-C_3	106.32
N_2-H_{25}	1.0119	C_1-N_2-H_{25}	122.58
C_3-C_4	1.4207	C_3-N_2-H_{25}	130.98
C_3-C_6	1.3916	N_2-C_3-C_4	104.54
C_4-N_5	1.3942	N_2-C_3-C_6	132.59
C_4-C_9	1.3967	C_4-C_3-C_6	122.85
C_6-C_7	1.3979	C_3-C_4-N_5	110.44
C_6-H_{26}	1.084	C_3-C_4-C_9	119.22
C_7-C_8	1.4139	N_5-C_4-C_9	130.32
C_7-O_{23}	1.3691	C_1-N_5-C_4	103.80
C_8-C_9	1.3922	C_3-C_6-H_{26}	123.39
C_8-H_{27}	1.0828	C_7-C_6-H_{26}	119.81
C_9-H_{28}	1.0849	C_6-C_7-O_{23}	114.98
S_{10}-O_{11}	1.5181	C_7-C_8-C_9	121.01
S_{10}-C_{12}	1.8552	C_4-C_9-H_{28}	120.36
C_{12}-C_{13}	1.5108	C_1-S_{10}-O_{11}	102.42
C_{12}-H_{29}	1.0959	C_1-S_{10}-C_{12}	93.598
C_{12}-H_{30}	1.0963	O_{11}-S_{10}-C_{12}	110.04
C_{13}-C_{14}	1.4085	S_{10}-C_{12}-C_{13}	111.08
C_{13}-N_{18}	1.3355	C_{13}-C_{12}-H_{29}	112.96
C_{14}-C_{15}	1.4019	H_{29}-C_{12}-H_{30}	108.02
C_{14}-C_{20}	1.5077	C_{12}-C_{13}-C_{14}	120.53
C_{15}-O_{21}	1.3799	C_{14}-C_{13}-N_{18}	123.30
C_{16}-C_{17}	1.3948	C_{13}-C_{14}-C_{15}	116.56
C_{16}-C_{19}	1.5061	C_{14}-C_{15}-O_{21}	119.86
C_{17}-N_{18}	1.336	C_{15}-C_{16}-C_{19}	121.78
C_{17}-H_{31}	1.0888	C_{16}-C_{17}-N_{18}	124.16
C_{19}-H_{32}	1.0964	C_{16}-C_{17}-H_{31}	119.78
C_{19}-H_{33}	1.0935	H_{33}-C_{19}-H_{34}	108.68
C_{19}-H_{34}	1.093	C_{14}-C_{20}-H_{35}	111.19
C_{20}-H_{35}	1.0948	H_{35}-C_{20}-H_{37}	106.84
C_{20}-H_{36}	1.0906	C_{15}-O_{21}-C_{22}	114.79
O_{21}-C_{22}	1.4298	O_{21}-C_{22}-H_{39}	111.53
C_{24}-H_{41}	1.0911	C_7-O_{23}-C_{24}	118.65
C_{24}-H_{42}	1.0977	O_{23}-C_{24}-H_{41}	105.92
C_{24}-H_{43}	1.0976	H_{41}-C_{24}-H_{42}	109.05

are longer than C-H bond lengths. The calculated geometrical parameter represent a good approximation and they are the basic for calculating the vibrational frequencies and thermodynamic parameter.

4.2 Vibrational assignments

The main objective of the vibrational analysis is to find the vibrational modes connected with the specific molecular structures of the calculated. The observed and calculated wavenumbers along with the relative intensities, probable assignments and total energy distribution (PED) are presented in Table 2. The experimental and theoretical FT-IR and FT-Raman spectra are shown in Fig2 and 3. The scale factor of 0.963 for B3LYP/6-31G (d, p) is used in the present work.

C-H vibrations

It is well known from literature that the C-H stretching, C-H in-plane bending and C-H out-of-plane bending vibrations usually appear in 2900-3150, 1100-1500 and 750-1000cm^{-1}respectively [8]. In the title compound C-H stretching vibration is observed at 3165 cm^{-1} at theoretically. C-H in plane bending vibration is observed at 1476 cm^{-1} in FT-IR and theoretically. C-H out of plane bending vibration is observed at 996 cm^{-1} in FT-Raman and 987 cm^{-1} in theoretically respectively. This also shows good agreement with the experimental and theoretical values as given in Table 2.

Table 2: Vibrational assignments obtained for S5M4M35DM3B at B3LYP/6-31G(d,p) basis set

Experimental		Theoretical	PED%
FT-IR	FT-Raman		
-	-	3628	vNH(99)
-	-	3229	vCH (87)+vCH (13)
-	-	3220	vCH (99)
-	-	3208	vCH (13)+vCH (86)
-	-	3164	vCH (99)
-	-	3156	vCH (87)
-	-	3148	vCH (87)
-	-	3146	vCH (91)
-	-	3138	vCH (43) + vCH (56)
-	-	3108	vCH (57) + vCH (42)
-	-	3106	vCH (38) + vCH (38) + vCH(24)
-	-	3096	vCH (64) + vCH (32)
-	3085	3087	vCH (52) + vCH (46)
-	-	3075	vCH (49) + vCH (51)
-	-	3052	vCH (43) + vCH 57
-	-	3041	vCH (25) + vCH(11) + vCH(63)
2992	3000	3014	vCH (47) + vCH(44)
1678	-	1688	vCC (21) + vCC (17) +vCC (12)+vCC (14)+vNC (11)
-	-	1639	vNC (13) + vCC (11) + vCC (30) + vCC (11)
1610	-	1628	vCC (11)+ δCCN(12)+δCCC(13)+ δCNC(10)
1592	-	1612	vNC (21) + vCC (27)+ δCCC (14)
1572	1571	1553	vNC (12) +δHCC(12)
-	-	1533	vNC (37) + vCC (12) + vCC (23)
-	-	1522	δHCH (41)
-	-	1520	δHCN(14)+ δHCH(10)+ δHCH (20)
-	-	1518	δHCH (11)+ δHCH (12)+ δHCH (50)
-	-	1511	δHCH (31)+ δHCH (28)+ τHCCC (11)
-	-	1502	δHCH (57)+ δHCH (15)+ τHCOC (12)
-	-	1501	δHCH (14)+ δHCH (37)
-	-	1492	vCC (10)+ δHCH (26) + δHCH (25) + δHCH (16)
-	-	1491	δHCH (17) + δHCH(38)+ δHCH (13)+ τHCCC(10)
1476	-	1476	vNC (15) + vCC (11) + δHCC (13) + δHCC (20)
-	-	1470	δHCN (12) +δHCH (11)
-	1448	1447	δHCH (73)
1435	-	1433	δHCH (12) +δHCH (30)+δHCH (14)
-	-	1426	vCC (13)+ δHCH (10)
-	-	1421	δHCH (23) +δHCH(20)+δHCH (25)
1401	-	1418	vNC (36) + δHNC(31)
-	1367	1383	vCC (20) + vCC (20)+δCCN (10)
-	-	1327	vNC (14)+vCC (10)+vCC (10)+vNC (15)+vOC (18)+ δHCC(13)+δHCN(19)
-	-	1313	vNC (12) + vNC (10) +vCC (17) +δHCN (27)
-	-	1301	vNC (16) + vNC (15) + vOC (13) + vCC (19)
1296	-	1299	vCC (10) +δHCC(12)+ vNC (27) + δHCC (18)
1272	-	1257	vNC(18)+ τHCCC (16) + τHCCC (13)
-	1251	1254	vNC (17) + vOC (11) + δHCC (13)
-	-	1239	vOC(17) + τHCCC (10)
1227	-	1232	vNC(15) + δHCC(30)
-	1210	1205	δHC(16) +τHCOC (28)+ τHCOC (24)
1197	-	1204	δHCH (13) + τHCOC (22)+ τHCOC (22)
-	-	1176	δHCC(65)+ τHCCC (11)
1151	1154	1155	vCC (11) + δHCC (20) + δHCC (27)
-	-	1135	vNC (17) + δHNC (34)
1115	1114	1102	vCC (12) + vOC (24)
1076	-	1070	vOC (47) + δHCC(13)
-	-	1068	δHCH (12)+ τHCCC (18) + τHCCC(27)
-	-	1053	τHCCC(19)+ τHCCC(10)
1030	-	1048	vSO (77)
1013	-	1036	vOC (52)
-	996	987	vCC (10)+vCC (14)+vCC (13)+τHCCC(17)
953	954	952	δCCC(22)+ δCNC (13)+ δNCN (14)
-	890	889	δNCC(12)+τHCCC(12)
-	852	845	τHCCC (68)+ γOCCC (16)
825	-	814	τHCCC (51) +τHCCC (25)
797	-	786	γOCCC(21)+ γOCCC (11)
762	763	765	vOC(15) +δCNC (30)+ δCNC (11)

-	-	755	τHCCC (13) +τHCCC(15)+τCCCC (15)+ γCNCC(28)
-	732	731	νSC (33)+δCNC (11)+ δSCC(11)
-	695	692	γNSNC(50)+ νSC (10) + τHNCC(13)
-	663	667	νCC(10)+ τCNCC(11)
636	620	638	γOCCC(17)+ τHCCC(11)
574	-	572	δCCC(16) + δCCC(17)+δCOC(16)
522	549	528	γCCCC (24)+ γCCCC (13)
-	512	506	νCC (11)+ δCCC(25)
-	412	403	γCCNC(14) +τCCCN(10)
-	321	320	γCCCC (14) +γCCCC (10)+γfCCNC (23)
-	252	258	τHCOC(24)+τHCOC (13)+τHCOC (13)+τCNCS(10)
-	217	224	δOSC(30)
-	126	121	δNCS (15)
-	69	64	τCCCN (14)+τCOCC(45)

ν– Stretching; δ–Bending; τ– Torsion; γ– Out of Plane Deformati

CH_3 vibrations

Methyl groups are generally referred as electron donating substituent's in the aromatic ring system. For CH_3 compound the mode appear in the region 2962–2872cm^{-1} are assigned to CH_3 stretching mode of vibrations [9,10]. In the title compound CH_3 vibrations is observed at 2992cm^{-1} in FT-IR, 3000 cm^{-1}n FT-Raman and 3014 cm^{-1} theoretically respectively as shown in Table 2. In general, the aromatic CH_3 stretching vibration calculated theoretically are in good agreement with the experimental values.

C-N vibrations

The identification of C-N vibration is a very difficult task, since the mixing of several bands is possible in this region. The C-N stretching vibrations generally occur in the region 1180–1280 cm^{-1}[9]. The C-N vibrations is observed at 1251 cm^{-1} in FT-Raman and 1254cm^{-1} theoretically respectively.

S-O Vibrations

The S-O vibrations absorb strongly at 1170–1155 cm^{-1}[9]. In the present investigation, a band observed at 1245 cm^{-1} in FT-IR is due to S-O stretching vibration. The theoretically calculated values are 1155 cm^{-1} by B3LYP method with 6-31G(d,p) basis sets respectively also shows good agreement with the experimentally recorded data as presented in Table 2.

C-S vibrations

In general, the assignment of the band due to C-S stretching vibrations for different compounds is difficult. On Because of the mixing of several bands, the identification of C-S vibrations is a very difficult task. The stretching vibrations assigned to the C-S linkage assigned occur in the region 700–600 cm^{-1}[11] and 775–650 cm^{-1}[9]. The C-S vibrations are found at 695 and 732 cm^{-1} in FT-Raman. The theoretically calculated values are 692 and 731 cm^{-1} by B3LYP level with 6-31G(d,p) basis set respectively and the values are in good agreement with the experimental values as presented in Table 2.

4.3 NBO analysis

The NBO studies a basic for exploring charge transfer or conjugative interaction in molecular systems and is an efficient method to know about intra- and intermolecular bonding and interaction among bonds. The NBO analysis has been performed on the molecule at the B3LYP/6-31(d,p) and summary of electron donor orbital, acceptor orbital and the interaction stabilization energy that resulted from the second-order perturbation theory is reported in Table 3. The larger value of E(2) gives the stronger interaction between electron donors (i) and electron acceptor (j) and reflects a more donating tendency from electron donor to electron acceptor and

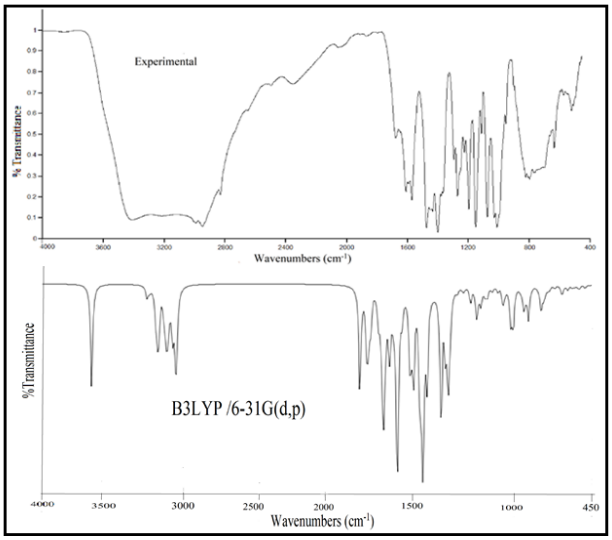

Fig.2 *The observed experimental & theoretical FT-IR spectra.*

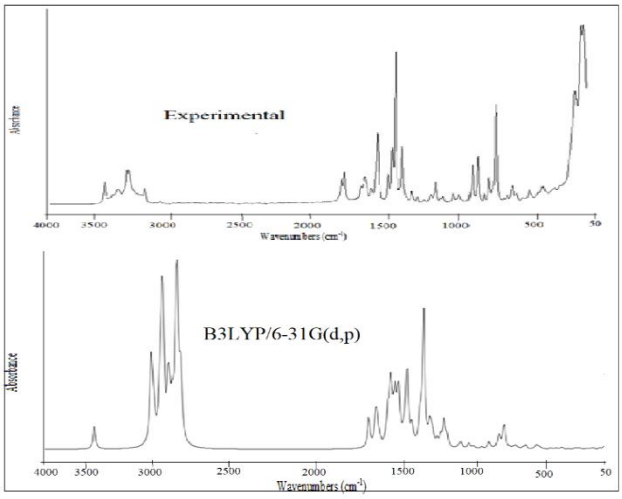

Fig.3 *The observed experimental & theoretical FT-Raman spectra.*

consequently a greater degree of conjugation of the whole system. Delocalisation of the electron density between occupied Lewis-type (bond or lone pair) NBO orbital and formally unoccupied (antibond and Rydgberg) non Lewis NBO orbital, corresponds to a stabilizing donar acceptor

interaction. In the title molecule, the intra-molecular interactions are due to the orbital overlap between bonding πC_{13}-N_{18}, π^*C_{14}-$C_{15}$and πC_{14}-C_{15}, π^*C_{13}-N_{18}leading to stabilization of 13.91 and 18.59 kJ/mol, respectively. The hybrid directionality and bond bending analysis of natural hybrid orbitals (NHOs) provides a clue of the substituent effect and steric effect. The intramolecular interaction are formed by the orbital overlap between bonding C-N and C-C antibond orbital which results intramolecular charge transfer (ICT) causing stabilization of the system. The lone pair interaction LP(1) C_4, LP(3) $O_{11}$with anti bonding orbital π^*C_1-N_5andσ^*S_{10}-C_{12}leading to stabilization of 58.04 and 10.82kJ/mol, respectively, is an evidence for charge transfer from the title compound.

Table 3. *Second order perturbation theory analysis of Fock matrix in NBO basis.*

Donor (i)	Acceptor (j)	E(2) kcal/mol	E(j)-E(i) a.u.	F(i,j) a.u.
πC_1-N_5	LP(1)C_4	27.83	0.21	0.095
πN_2-C_3	LP(1)C_4	11.46	0.22	0.061
πN_2-C_3	π^*C_1-N_5	30.06	0.32	0.093
πC_6-C_7	π^*N_2-C_3	38.03	0.21	0.091
πC_6-C_7	π^*C_8-C_9	16.61	0.28	0.062
πC_8-C_9	LP(1)C_4	41.52	0.14	0.087
πC_8-C_9	π^*C_6-C_7	21.88	0.27	0.071
πC_{13}-N_{18}	π^*C_{14}-C_{15}	13.91	0.32	0.060
πC_{13}-N_{18}	π^*C_{16}-C_{17}	22.96	0.32	0.078
πC_{14}-C_{15}	π^*C_{13}-N_{18}	27.00	0.26	0.076
πC_{14}-C_{15}	π^*C_{16}-C_{17}	18.77	0.29	0.067
πC_{16}-C_{17}	π^*C_{13}-N_{18}	18.59	0.26	0.062
πC_{16}-C_{17}	π^*C_{14}-C_{15}	22.42	0.27	0.070
LP(1) C_4	π^*C_1-N_5	58.04	0.10	0.079
LP(1) C_4	π^*N_2-C_3	250.99	0.07	0.119
LP(1) C_4	π^*C_8-C_9	73.19	0.14	0.108
LP(3) O_{11}	σ^*S_{10}-C_{12}	10.82	0.28	0.049
LP(2) O_{23}	π^*C_6-C_7	26.46	0.32	0.088
π^*N_2-C_3	π^*C_1-N_5	53.27	0.03	0.048
π^*N_2-C_3	π^*C_6-C_7	93.14	0.07	0.094
π^*C_{13}-N_{18}	π^*C_{14}-C_{15}	187.91	0.02	0.086
π^*C_{13}-N_{18}	π^*C_{16}-C_{17}	105.95	0.03	0.078

[a] *E(2) means energy of hyper conjugative interaction (stabilization energy).*
[b] *Energy difference between donor and acceptor i and j NBO orbitals.*
[c] *F(i, j) is the fork matrix element between i and j NBO orbitals.*

4.4 Mulliken charge analysis and Natural population analysis

In genereal, the calculation of atomic charges plays an most important role in the application of quantum mechanical calculations to molecular analysis [12].The Mulliken charge and Natural population analysis are calculated at B3LYP/6-31G(d,p) level is given in Table 4 and Fig.4. These charges are expected to influence the properties like dipole moment, electronic parameters, polarizability, and refractivity [13,14]. All hydrogen atoms have positive charges ranging from 0.5251 to 0.7852eV. The carbon atoms in the double ring carry both positive and negative charges. The substituted Sulphur has positive charge whereas carbon and oxygen atoms have negative charges.

Table 4.*Mulliken atomic charges and NPA of the title compound*

Atoms	B3LYP/6-31G(d,p)	
	Mulliken	NPA
C_1	0.1778	5.8130
N_2	-0.6059	7.5795
C_3	0.3292	5.8656
C_4	0.1991	5.9238
N_5	-0.5200	7.4883
C_6	-0.1479	6.3009
C_7	0.3431	5.6937
C_8	-0.1489	6.3305
C_9	-0.1223	6.2120
S_{10}	0.8765	14.936
O_{11}	-0.6525	8.8505
C_{12}	-0.4746	6.6195
C_{13}	0.2452	5.8163
C_{14}	0.1091	6.0709
C_{15}	0.2586	5.6761
C_{16}	0.0949	6.0844
C_{17}	0.0485	5.9877
N_{18}	-0.4797	7.4534
C_{19}	-0.3793	6.7157
C_{20}	-0.3928	6.7263
O_{21}	-0.5350	8.5617
C_{22}	-0.0810	6.3446
O_{23}	-0.5270	8.5247
C_{24}	-0.0771	6.3556
H_{25}	0.2866	0.5251
H_{26}	0.0899	0.7355
H_{27}	0.0866	0.7526
H_{28}	0.1035	0.7435
H_{29}	0.1776	0.7152
H_{30}	0.1590	0.7219
H_{31}	0.1026	0.7584
H_{32}	0.1280	0.7512
H_{33}	0.1307	0.7338
H_{34}	0.1177	0.7487
H_{35}	0.1178	0.7445
H_{36}	0.1306	0.7318
H_{37}	0.1318	0.7465
H_{38}	0.1238	0.7593
H_{39}	0.1164	0.7863
H_{40}	0.1122	0.7854
H_{41}	0.1190	0.7562
H_{42}	0.1076	0.7858
H_{43}	0.1199	0.7852

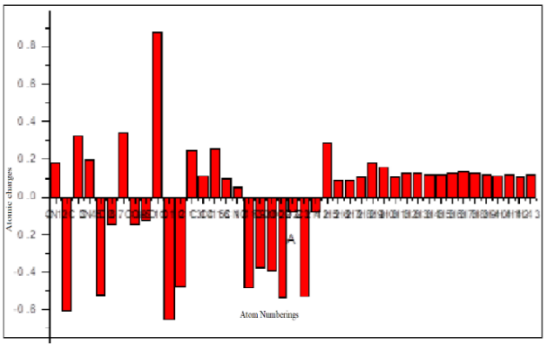

Fig 4.*Mulliken atomic charges of S5M4M35DM3B*

The NPA and Mulliken charge values shows that the presence of three nitrogen atoms, three oxygen atoms and one sulphur atom. However, sulphuratom possess large

positive charges. Moreover, there is hardly any difference in charge distribution observed on all hydrogen atoms.

4.5 UV–visible and FMO analysis

Normally the electronic transitions occurs in the organic molecules are π→π*, n→π*, π* (acceptor) →π (donor) [15,16]. The major contributions of transitions were calculated with the help of Gauss View Program [17]. The recorded UV–Vis absorption spectrum of S5M4M35DM3B molecule was shown in Fig. 5. The calculated absorption peak (λ_{max}), vertical excitation energies, oscillator strength (f) by B3LYP/6-31G(d,p) method were tabulated in Table 5 and Table 6. Oscillator strength f is a dimensionless quantity which describes the strength of an electronic transition. Transitions with extremely low or zero f values are forbidden. Excitation of 277.99 nm has low oscillator strength. Only slight variation is observed experimentally. The HOMO energy denote the ability of give electrons and LUMO denote the ability to accept the electrons, the gap between HOMO and LUMO characteristic the molecular chemical stability [18] .The energy gap between HOMO and LUMO is 8.14770eV is shown in Fig 6 . The energy gap between HOMO and LUMO has been proving that bioactivity from intermolecular charge transfer [19,20].

$I = - E_{HOMO}$ and $A = - E_{LUMO}$.

The absolute hardness of the molecule is

$(\eta) = (I-A)/2.$ (1)

The softness is the inverse of the hardness

$(S) = 1/\eta.$ (2)

The chemical potential of the molecule is

$(\mu) = - (I +A)/2.$ (3)

The electrophilicity index of the molecule is

$(\omega) = \mu^2/2\eta.$ 4)

The electronegativity of the molecule is

$(\chi) = (I+A)/2.$ (5)

The values of ionization potential, electron affinity, chemical hardness, softness, chemical potential, electrophilicity and electro negativity are 8.80431, 0.65661, 4.07385, 0.24546, -4.7304, 4.73046, 11.1886 eV calculated at B3LYP level with B3LYP/6-31G(d,p) basis sets respectively for the title molecule.

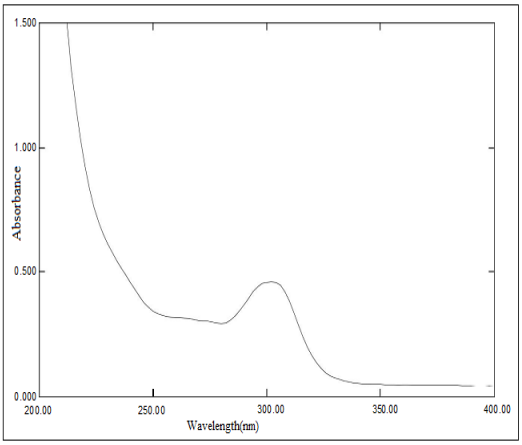

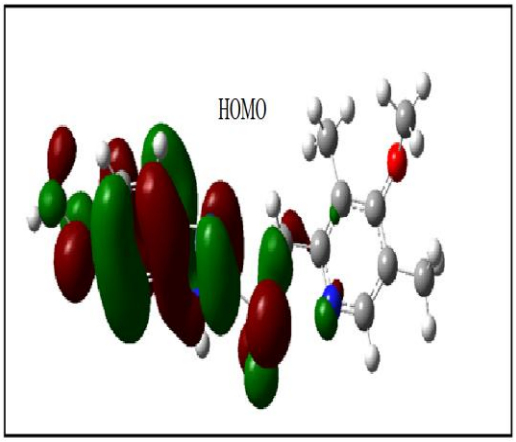

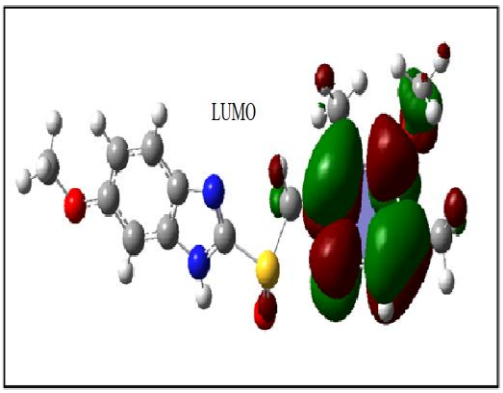

Fig.5, 6 & 7. *The observed experimental UV spectra.Frontier molecular orbital of S5M4M35DM3B*

4.6 Molecular Electrooststic Potential

The Molecular electrostatic potential (MEP) is very useful in the investigation of the molecular structure with its physiochemical property relationships [21-14]. The molecular electrostatic potential surface (MEP) is a method of mapping electrostatic potential onto the iso-electron density surface simultaneously displays electrostatic potential distribution, molecular shape, size and dipole moments of the molecule and it plays an vital role in visual method to understand the relative polarity [25]. The total electron density and MEP surfaces of the molecules under investigation are constructed by using B3LYP/6-31G(d,p) method. MEP is very useful in understanding the sites of electrophilic and nucleophilic attacks reaction for the study

of the biological process [26] and hydrogen bonding interactions [27,28]. The negative such as red and yellow regions of MEP were related to electrophilic reactivity and the positive such as blue regions to nucleophilic reactivity. The resulting potential surface simultaneously displays molecular size and shape and electrostatic potential value. The different values of the electrostatic potential at the surfaces are represented by different colors. The Potential increasing order will be red < orange < yellow < green < blue. Molecular electrostatic potential of S5M4M35DM3B is shown in Fig. 7

4.7 Local reactivity descriptors

Local quantities such as Fukui functionf(r) and local softness s(r) defined the reactivity/selectivity of a specific site in a molecule. The Fukui function is defined as the first derivative of the electronic density ρ(r) of a system with respect to the number of electrons N at a constant external potential v(r) [29]

$$.f(r) = \left[\frac{\partial\rho(r)}{\partial N}\right]_{v(r)} = \left[\frac{\delta\mu}{\delta v(r)}\right]_N \quad (6)$$

Using left and right derivatives with respect to the number of electrons, electrophilic and nucleophilic Fukui functions for a site k in a molecule can be defined [30].

Table 5. The UV–Vis excitation energy of the title compound

States	Experimental λ_{abs}	Singlet - A	B3LYP/6-31G(d,p)		
			λcal	Frequency (f)	E(eV)
Excited state 1 90 →92 91 →92	320	0.17986 0.62716	295.42	0.4258	4.1969
Excited state 2 90 → 93 91 → 93	302	0.17173 0.66612	285.29	0.0001	4.3459
Excited state 3 90 → 94 91 →94	280	0.16183 0.66451	277.99	0.0272	4.4600

Table 6. *Molecular properties of Esomeprazole*

Molecular properties	B3LYP 6-31G(d,p)	Molecular properties	B3LYP 6-31G(d,p)
E_{HOMO}(eV)	-8.80431	Chemical Hardness(η)	4.07385
E_{LUMO}(eV)	-0.65661	Softness(S)	0.24546
$E_{Homo-Lumo}$gap(eV)	8.14770	Chemical Potential(μ)	-4.7304
Ionisation potential(I) eV	8.80431	Electronegativity(χ)	4.73046
Electron affinity (A) eV	0.65661	Electrophilicity index(ω)	11.1886

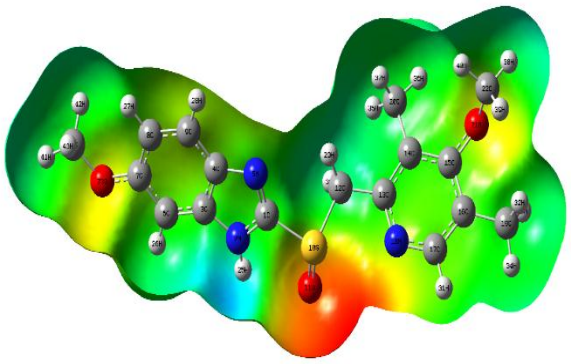

Fig.7 *Molecular electrostatic potential of S5M4M35DM3B*

$f_k^+ = [\rho_{k(N+1)}-\rho_{k(N)}]$ for nucleophilic attack (7)
$f_k^- = [\rho_{k(N)}-\rho_{k(N-1)}]$ for electrophilic attack (8)
$f_k^0 = [\rho_{k(N+1)}-\rho_{k(N-1)}]/2$ for radical attack (9)

where$\rho_{k(N)}$, $\rho_{k(N-1)}$ and $\rho_{k(N+1)}$ are the gross electronic populations of the site k in neutral, cationic, and anionic systems, respectively. Regioselectivity of these polar reactions has been well explained identifying the more electrophilic center through the local electrophilicity, ω_k^+, whereas the f_k^-index multiplied by the total softnessor the global electrophilicity[31,32]has been used to identifythe more nucleophilic center of a molecule.More recently, Pérez et al. [33]extended the nucleophilicity model at the selectivity regime by using a new defining of the local nucleophilicity index based on the nucleophilic Fukui function, f_k^-. According to these authors, the global nucleophilicity index N, can be expressed as the sum of local nucleophilicities condensed to all atoms of the molecule:

$N = \Sigma N_k$ (10)

From the above definition of the global nucleophilicity, it is possible to define the local nucleophilicity condensed to an atom k through the nucleophilic Fukui function, f_k^-.

$N_k = Nf_k^-$ (11)

This new index defining the local nucleophilicity will be used in this work for the prediction of the favored site of the five-membered heterocycles in electrophilic aromatic substitutions. The most relevant local descriptor of reactivity is the Fukui function. Yang and Parr [34] proposed a finite difference to calculate Fukui function indices. In a molecular system, f_k^+ measures the change in density when the molecule gains electrons and it corresponds to reactivity

with respect to nucleophilic attack. Whereas, f_k^- corresponds to reactivity with respect to electrophilic attack when the molecule losses electrons. In addition to fukui function the local softness (S_k^+, S_k^-, S_k^0) is also used to describe the reactivity of the molecular system. Fukui function and local softness for selected atomic sites in S5M4M35DM3B have been listed in the Table 7. From the values reported in the Table 9, the highest nucleophilic attack is on S_{10}. The other nucleophilic attack order was found to be S_{10}> H_{26}> H_{27}> H_{28}> H_{41} >C_6. The sites for electrophilic attack were $S_{10,}$ H_{28}, and O_{11}. The radial attack was on H_{26}, S_{10} and O_{23}. S_k^+, S_k^- and S_k^0 predicts the most nucleophilic and electrophilic and radial attack in a molecule is the one which has the $S_k^{+,-/0}$ value, in turn is the softest region in a molecule.

4.8.Molecular docking study

The molecular docking analysis [35] was carried out for the moleculeS5M4M35DM3B with targeted proteins which have the properties of antiulcer activity. The selected proteins properties were predicted using an online tool PASS (Prediction of Activity of Spectra for Substances) with active site of Pa (Probability to be Active) is greater than four (Pa > 4) and the structures of the targeted proteins were obtained from the PDB ID format. The ligand PDB IB file was created by using the optimized geometric structure of the title molecule. The AutoDockTools graphical user interface was used to remove the ligand and water molecules present in the targeted proteins. Polar hydrogen bond and Kollman charges were added and then Lamarckian Genetic Algorithm (LGA) was used for molecular docking calculations in the AutoDock 4.0 software [36-38]. The interaction between the ligand and the targeted proteins are presented in Fig. 8. And Table 8 shows the interaction energies that occur when ligand bind to the protein.In this study, we can understand the transport of small molecule called ligand in biological systems. Auto Dock suite 4.2.6 is an excellent tool to get insights into the molecular mechanism of ligand-protein interactions bind to a receptor of the well known three-dimensional structure. The optimized structure is obtained from Gaussian 03 was docked using Auto Dock Tools. S5M4M35DM3B was selected to be docked at the active areas of receptor 1AFC of antiulcer proteins which were downloaded from the protein data bank (RCSB). Hundred docking runs are used to obtain the best-fit proteins and it has very lowest binding energy. The inhibition constants (mm) and molecular docking binding energies (kcal/mol) were obtained. Among them, 1AFC shows the lowest energy of binding at -5.56 kcal/mol and most docked inhibitors interacted with the ligand. This protein has one residue hydrogen bonds having SER 117 with bond distance 2.1 Å. The 1AFC ligand interacts with different receptors. This lower binding energy shows the antiulcer protein 1AFC is properly bound with S5M4M35DM3B.

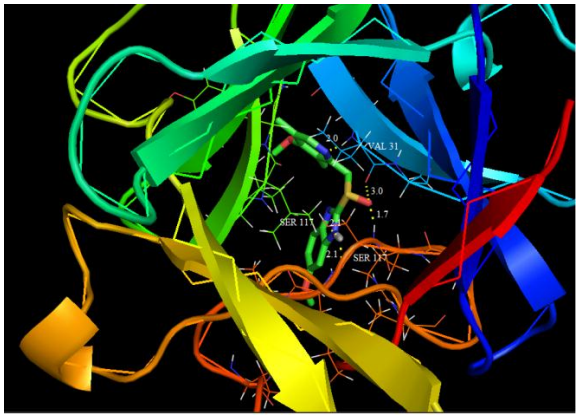

Fig 8. *Docking and Hydrogen bond interactions of S5M4M35DM3B with 1AFC protein.*

Table 7*.Condensed Fukui functions and local softness of the title compound*

Atoms	f_k^+	f_k^-	f_k^0	Sf_k^+	Sf_k^-	Sf_k^0
C_1	0.03542	0.02968	0.03254	0.00869	0.00728	0.00798
N_2	0.01442	0.00502	0.00972	0.00354	0.00123	0.00238
C_3	0.00728	0.02097	0.01413	0.00178	0.00514	0.00346
C_4	0.03939	-0.01761	0.01088	0.00966	-0.00432	0.00267
N_5	0.03660	0.05709	0.04685	0.00898	0.01401	0.01150
C_6	0.04142	0.03090	0.03616	0.01016	0.00758	0.00887
C_7	0.02738	0.02603	0.02670	0.00672	0.00638	0.00655
C_8	0.02480	0.00553	0.01517	0.00608	0.00135	0.00372
C_9	0.03626	0.02945	0.03285	0.00890	0.00722	0.00806
S_{10}	0.08077	0.07176	0.07627	0.0198	0.01761	0.01872
O_{11}	0.09610	0.02476	0.06043	0.02359	0.00607	0.01483
C_{12}	-0.00290	-0.03526	-0.01908	-0.00071	-0.00865	-0.00468
C_{13}	-0.00236	0.02496	0.01129	-0.00058	0.00727	0.00277
C_{14}	0.00934	0.01819	0.01376	0.00229	0.00446	0.00337
C_{15}	0.01827	0.06434	0.04130	0.00448	0.01579	0.01013
C_{16}	0.02132	-0.02371	-0.00119	0.00523	-0.00582	-0.00029
C_{17}	0.01639	0.04402	0.03020	0.00402	0.01080	0.00741
N_{18}	-0.00826	0.04108	0.01641	-0.00202	0.01008	0.00402
C_{19}	-0.02405	0.01177	-0.00613	0.00590	0.00289	-0.00150
C_{20}	-0.00821	-0.00787	-0.00804	-0.00201	-0.00193	-0.00197
O_{21}	0.01200	0.00804	0.01002	0.00294	0.00197	0.00246
C_{22}	-0.00821	-0.02731	-0.01776	-0.00201	-0.00670	-0.00436
O_{23}	0.06383	0.01302	0.03843	0.01566	0.00319	0.00943
C_{24}	-0.03907	-0.02714	-0.03309	-0.00959	-0.00666	-0.00812
H_{25}	0.02531	0.03418	0.02974	0.00621	0.00839	0.00730
H_{26}	0.07185	0.04844	0.06014	0.01763	0.01189	0.01476
H_{27}	0.05957	0.05293	0.05625	0.01462	0.01299	0.01380
H_{28}	0.05997	0.06300	0.06148	0.01472	0.01546	0.01509
H_{29}	0.01299	0.02518	0.01909	0.00318	0.00618	0.00468
H_{30}	0.03815	0.02598	0.03207	0.00936	0.00637	0.00787
H_{31}	0.02521	0.05256	0.03888	0.00618	0.01290	0.00955
H_{32}	0.01360	0.03004	0.02182	0.00333	0.00737	0.00535
H_{33}	0.01700	0.02283	0.01992	0.00417	0.00560	0.00488
H_{34}	0.01927	0.02156	0.02041	0.00473	0.00529	0.00501
H_{35}	0.01976	0.01094	0.01534	0.00485	0.00268	0.00376
H_{36}	0.02201	0.03343	0.02772	0.00540	0.00820	0.00680
H_{37}	-0.01645	0.02990	0.00672	-0.00403	0.00734	0.00165
H_{38}	0.02096	0.03719	0.02908	0.00514	0.00912	0.00713
H_{39}	-0.00197	0.02618	0.01407	0.00048	0.00642	0.00345
H_{40}	-0.00018	0.01986	0.00983	-0.00004	0.00487	0.00241
H_{41}	0.05079	0.03359	0.04219	0.01246	0.00824	0.01035
H_{42}	0.04052	0.01627	0.02840	0.00994	0.00399	0.00697
H_{43}	0.02966	0.02811	0.02888	0.00728	0.00690	0.00709

Table 8. *Hydrogen bonding and molecular docking with ulcer protein target*

Protein (PDB ID)	Bonded residues	No. of hydrogen bond	Bond distance(Å)	Estimated Inhibition Constant(μm)	Binding energy (kcal/mol)	Reference RMSD(Å)
1AFC	SER 117	5	2.1	70.63	-5.56	15.97
	SER 117		2.1			
	SER 117		1.7			
	VAL 31		3.0			
	VAL 31		2.0			

5. Conclusion

In the present work, the geometry of the title compound S5M4M35DM3B was optimized with DFT-B3LYP method using 6-31G(d,p) basis set. The molecular structural parameters like bond length and bond angle, Mulliken Atomic charges and vibrational frequencies of the fundamental modes of the optimized geometry have been determined from DFT calculations. The complete vibrational assignments of wave numbers are made on the basis of potential energy distribution (PED). Close agreement between the experimental and theoretical frequencies were achieved. HOMO-LUMO energy gap has

been calculated. The MEP analysis reveals the sites for electrophilic attack and nucleophilic reactions. The formation of hydrogen bond was investigated in terms of the charge density by the NBO calculations. The electronic structure and the assignments of the absorption bands were made by the UV spectra and TD-DFT calculations. Fukui function shows the nucleophilic and electrophilic attacking sites are determined.We believe that the results of this study will be of assistance to those who are in the pursuit of experimental and theoretical details of the title molecule. From the Molecular docking studies, the active site of the ulcer protein targeted have been determined.

REFERENCES

[1]. [Laine L. Approaches to nonsteroidal anti-inflammatory drug use in the highrisk patient. Gastroenterology 2001; 120: 594–606.

[2]. Scheiman JM. Prevention of NSAID induced ulcers. Curr Treat Options Gastroenterol 2008; 11: 125–34.

[3]. Lanza FL, Chan FK, Quigley EMM. Guidelines for prevention of NSAID related ulcer complications. Am J Gastroenterol 2009; 104: 728-38.

[4]. A.D.Becke, J.Chem. Phys. 98(1993)5648-5652.

[5]. C.Lee, W.Yang, R.G.Parr, Phys. Rev. B 37(1988)785-789.

[6]. M.J.Frisch, G.W.Trucks, H.B.Schlegel, G.E.Scuseria, M.A.Robb, J.R.Cheeseman, J.A.Montgomery, T.Vreven, K.N.Kudin, J.C.Burant, J.M.Millam, S.S.Iyengar, J.Tomasi, V.Barone, B.Mennucci, M.Cossi, G.Scalmani, N.Rega, G.A.Petersson, H.Nakatsuji, M.Hada, M.Ehara, K.Toyota, R.Fukuda, J.Hasegawa, M.Ishida, T.Nakajima, Y.Honda, O.Kitao, H.Nakai, M.Klene, X.Li, J.E.Knox, H.P.Hratchian, J.B.Cross, V.Bakken, C.Adamo, J.Jaramillo, R.Gomperts, R.E.Stramann, O.Yazyev, A.J.Austin, R.Cammi, C.Pomelli, J.W.Ochterski, P.Y.Ayala, K.Morokuma, G.A.Voth, P.Salvador, J.J.Dannenberg, V.G.Zakrzewski, S.Dapprich, A.D.Daniels, M.C.Strain, O.Farkas, D.K.Malick, A.D.Rabuck, K.Raghavachari, J.B.Foresman, J.V.Ortiz, Q.Cui, A.G.Baboul, S.Clifford, J.Cioslowski, B.B.Stefanov, G.Liu, A.Liashenko, P.Piskorz, I.Komaromi, R.L.Martin, D.J.Fox, T.Keith, A.Laham, C.Y.Peng, A.Nanayakkara, M.Challacombe, P.M.W.Gill, B.Johnson, W.Chen, M.W.Wong, C.Gonzalez, J.A.Pople, Gaussian 03, Revision C.02,2003.

[7]. M.H.Jamróz, Spectrochim.Acta. A 114(2013)220.

[8]. L.J.Bellamy, The Infrared Spectra of Complex Molecules, vol. 2, Chapman and Hall, London, 1980.

[9]. M. Silverstein, G. Clayton Basseler, C. Morill, Spectrometric Identification of Organic Compound, Wiley, NewYork, 1981.

[10]. G. Socrates, Infrared Characteristic Group frequencies, Wiley-Interscience

[11]. Publication, New York, 1980.

[12]. B. Lambert, Introduction to Organic Spectroscopy, Macmillan Publjcation, New York, 1987. [12] S. Gunasekaran, S. Kumaresan, R. Arunbalaji, G. Anand, S. Srinivasan, J. Chem. Sci. 120 (2008) 315.

[13]. R.J. Xavier, P. Dinesh, Spectrochim. Acta A 118 (2014) 999–1011.

[14]. M. Govindarajan, M. Karabacak, V. Udayakumar, S. Periandy, Spectrochim. Acta 88 (2012) 37–48.

[15]. T. Shimanouchi, Y. kakiuti, I. Gam, J. Chem. Phys. 25 (1956) 1245–1251.

[16]. J.N. Liu, Z.R. Chen, S.F. Yuvan, J. Zhejang, Univ. Sci. B6 (2005) 584–590

[17]. H.M. Shiri, M. Ghaemi, S. Raihi, A.A. Sehat, Int. J. Electrochem. Sci. 6 (2011) 317–336.

[18]. K. Fukui, Science 218 (1982) 747–754.

[19]. L. Padmaja, C. Ravikumar, D. Sajan, I.H. Joe, V.S. Jayakumar, G.R. Petti, O.F.Nelson, J. Raman Spectrosc. 40 (2009) 419–428.

[20]. C. Ravikumar, I.H. Joe, V.S. Jayakumar, Chem. Phys. Lett. 460 (2008) 552–558.

[21]. I. Fleming, Frontier Orbitals and Organic Chemical Reactions, John Wiley & Sons, New York, (1976) 5–27.

[22]. J.M. Seminario, Recent Developments and Applications of Modern Density Functional Theory, vol.4, Elsevier, 1996.

[23]. T. Yesilkaynak, G. Binzet, F. Mehmet Emen, U. Florke, N. Kulcu, H. Arslan, Eur. J. Chem. 1 (2010) 1–5.

[24]. P. Politzer, P.R. Laurence, K. Jayasuriya, J. McKinney, Environ. HealthPerspect. 61 (1985) 191–202.

[25]. P. Politzer, P. Lane, Struct. Chem. 61 (1990) 159–164.

[26]. E. Scrocco, J. Tomasi, Adv. Quantum. Chem. 103 (1978) 115–193.

[27]. F.J. Luque, J.M. Lopez, M. Orozco, Theor. Chem. Acc. 103 (2000) 343–345.

[28]. P. Politzer, J.S. Murray, in: D.L. Beveridge, R. Lavery (Eds.), Theoretical Biochemistry, and Molecular Biophysics: A Comprehensive Survey, Protein, vol. 2, Adenine Press, Schenectady, New York, 1991.

[29]. R.G. Parr, W. Yang, J. Am. Chem. Soc. 106 (1984) 4049.

[30]. W. Yang, W. Mortier, J. Am. Chem. Soc. 108 (1986) 5708.
L.R. Domingo, M. Arno, R. Contreras, P. Pérez, J. Phys. Chem. A 106 (2002) 952.

[31]. P.K. Chattaraj, B. Maiti, U. Sarkar, J. Phys. Chem. A 107 (2003) 4973.

[32]. P. Pérez, L.R. Domingo, M. Duque-Noreña, E. Chamorro, J. Mol. Struct. (THEOCHEM) 895 (2009) 86.

[33]. W.Yang, R.Parr, Proc. Natl. Acad. Sci (Chem.) 82 (1985) 6723-6726.

[34]. P. Sledz, A. Caflish, Protein structure-based drug design: from docking to molecular dynamics, J. Struct. Biol. 48 (2018) 93e102.

[35]. M. Sanner, Python: a programming language for software integration and development, J. Mol. Graph. Model.17 (1999) 57e61.

[36]. J.H. Holland, Adaptation in Natural and Artificial Systems, The University of Michigan Press, Ann Arbor, 1975.

[37]. M.W. Chang, R.K. Belew, K.S. Carroll, A.J. Olson, D.S. Goodsell, Empirical entropic contributions in computational docking: evaluation in APS reductase

[38]. complexes, J. Comput. Chem. 29 (2008) 1753e1761.